



THE UNIVERSITY *of* EDINBURGH

Edinburgh Research Explorer

West Antarctic Surface Climate Changes Since the Mid20th Century Driven by Anthropogenic Forcing

Citation for published version:

Dalaiden, Q, Schurer, AP, Kirchmeieryoung, MC, Goosse, H & Hegerl, GC 2022, 'West Antarctic Surface Climate Changes Since the Mid20th Century Driven by Anthropogenic Forcing', *Geophysical Research Letters*, vol. 49, no. 16, e2022GL099543. <https://doi.org/10.1029/2022GL099543>

Digital Object Identifier (DOI):

[10.1029/2022GL099543](https://doi.org/10.1029/2022GL099543)

Link:

[Link to publication record in Edinburgh Research Explorer](#)

Document Version:

Peer reviewed version

Published In:

Geophysical Research Letters

General rights

Copyright for the publications made accessible via the Edinburgh Research Explorer is retained by the author(s) and / or other copyright owners and it is a condition of accessing these publications that users recognise and abide by the legal requirements associated with these rights.

Take down policy

The University of Edinburgh has made every reasonable effort to ensure that Edinburgh Research Explorer content complies with UK legislation. If you believe that the public display of this file breaches copyright please contact openaccess@ed.ac.uk providing details, and we will remove access to the work immediately and investigate your claim.



1 **West Antarctic surface climate changes since the**
2 **mid-20th century driven by anthropogenic forcing**

3 **Quentin Dalaiden¹, Andrew P. Schurer², Megan C. Kirchmeier-Young³,**
4 **Hugues Goosse¹ and Gabriele C. Hegerl²**

5 ¹Université catholique de Louvain (UCLouvain), Earth and Life Institute (ELI), Louvain-la-Neuve,
6 Belgium

7 ²School of Geosciences, University of Edinburgh, United Kingdom

8 ³Climate Research Division, Environment and Climate Change Canada, Toronto, ON M3H 5T4, Canada

9 **Key Points:**

- 10 • Surface climate changes since the 1950s in West Antarctica are out of the range
11 of internal variability
- 12 • The increase in greenhouse gas emissions and stratospheric ozone depletion are
13 responsible for these changes
- 14 • The future changes over the 21st century will depend on both the greenhouse gas
15 emissions and the ozone layer recovery

Corresponding author: Quentin Dalaiden, quentin.dalaiden@uclouvain.be

Abstract

Although the West Antarctic surface climate has experienced large changes over the past decades with widespread surface warming, an overall increase in snow accumulation and a deepening of the Amundsen Sea Low, the exact role of human activities in these changes has not yet been fully investigated, which limits confidence in future projections. Here, we perform a detection and attribution analysis using instrumental and proxy-based reconstructions, and two large climate model simulation ensembles to quantify the forced response in these observed changes. We show that surface climate changes since the 1950s were driven by anthropogenic forcing, in particular the greenhouse gas forcing and stratospheric ozone depletion. Therefore, our results indicate that the 21st century changes will depend on both the greenhouse gas emissions and the ozone layer recovery.

Plain Language Summary

Since the second half of the 20th century, West Antarctica has experienced large climate changes, such as widespread warming, increased snow accumulation and a deepening of a low-pressure system located off the West Antarctic coasts. The observed climate changes in West Antarctica are influenced by both the internal (related to the chaotic nature of climate) and forced (related to changes in forcings) variability but it is still unclear to what extent human activities are responsible for these changes. We used a statistical method to distinguish between changes caused by humans and by natural influences both for instrumental observations and reconstructions of past climate. Our results show that the observed changes since the 1950s are out of the range of natural variability and can be attributed to human activities – i.e., the increase of greenhouse gases and stratospheric ozone depletion. Therefore, our findings indicate that the future state of the West Antarctic surface climate will depend on the greenhouse gas emissions as well as the ozone layer recovery.

1 Introduction

Over the past decades, the Antarctic has experienced large climate changes, in particular over the West Antarctic Ice Sheet (WAIS), situated in the Pacific Sector of the Southern Ocean (e.g., IPCC, 2019). The widespread atmospheric warming observed (e.g.,

46 Steig et al., 2009) there is associated with a snow accumulation increase over the Antarc-
47 tic Peninsula, Eastern and Central WAIS, and a snow accumulation decrease in West-
48 ern WAIS (Medley & Thomas, 2019). It has been shown that these changes are closely
49 related to modifications in the general atmospheric circulation (e.g., Marshall & Thomp-
50 son, 2016; Marshall et al., 2017; Thomas et al., 2015; Medley & Thomas, 2019; Dalaiden
51 et al., 2021), and in particular in the low-pressure system situated off the West Antarc-
52 tic coasts, referred to as the Amundsen Sea Low (ASL) (Turner et al., 2009; Raphael et
53 al., 2016; Hosking et al., 2013). Given the critical importance of the West Antarctic cli-
54 mate variability on the future global climate, better understanding the drivers of these
55 surface changes as well as the contribution from the forced and internal variability is cru-
56 cial for reducing uncertainties in climate projections.

57 Stratospheric ozone depletion has been identified as the main contributor to the
58 atmospheric circulation changes in the Southern Hemisphere, with a minor contribution
59 from the increase in greenhouse gas concentrations (Thompson et al., 2011; England et
60 al., 2016; Fogt & Zbacnik, 2014). Additionally, stratospheric ozone depletion may ac-
61 count for almost a third of the modelled Antarctic-wide snow accumulation increase over
62 1986–2005 (Lenaerts et al., 2018). Furthermore, the widespread post-1950s West Antarc-
63 tic atmospheric warming strongly suggests an important role of greenhouse gases (Steig
64 et al., 2009). Similarly, according to Medley and Thomas (2019), the overall warming
65 of the atmosphere may explain the 20th century Antarctic-wide snow accumulation. In
66 addition to the Gillett et al. (2008) study which attributed warming at both poles to an-
67 thropogenic forcing, two recent studies (Swart et al., 2018; Hobbs et al., 2021) have demon-
68 strated that the observed warming and freshening of the Southern Ocean since the 20th
69 century are inconsistent with internal variability of the climate alone and is mainly at-
70 tributed to the increased atmospheric greenhouse gas concentrations and ozone deple-
71 tion. Furthermore, the summer austral increase of the Southern Annular Mode (roughly
72 representing the position and intensity of the westerly winds (Fogt & Marshall, 2020))
73 since the 1950s is one of the unique atmospheric changes that has been attributed to a
74 forcing (Gillett et al., 2013; Jones et al., 2016). However, to our knowledge, no optimal
75 fingerprinting study exists of the ASL changes, and more generally of the West Antarc-
76 tic climate changes over the past decades.

77 This can be explained by the very sparse observational network (Turner et al., 2005)
78 and the strong internal climate variability in the West Antarctic (e.g., Connolley, 1997)

79 that make it complicated to detect a forced trend. However, over the past years, several
80 spatially complete datasets have been released describing the atmospheric circulation (Fogt
81 et al., 2019; Dalaiden et al., 2021; O’Connor et al., 2021), atmospheric temperature (Nicolas
82 & Bromwich, 2014) and snow accumulation (Medley & Thomas, 2019; Dalaiden et al.,
83 2021) in this region. In parallel, large ensembles (LEs) of Earth System Model (ESM)
84 simulations are becoming more common (Deser, Lehner, et al., 2020; Maher et al., 2021).
85 Single model LEs are built by performing several simulations with a single climate model
86 using the same forcing but initialized with slightly different initial conditions to estimate
87 the effect of internal variability. As a consequence, LEs allow comparing the contribu-
88 tion from the internal and forced variability on the simulated changes. LEs are partic-
89 ularly relevant for detection and attribution studies since the impact of unpredictable
90 internal variability is minimized with the average of the simulations (i.e., maximising the
91 signal-to-noise ratio). Additionally, some LEs provide single-forcing experiments, which
92 provide the opportunity to assess the impact of a specific forcing.

93 In this study, we aim at detecting and attributing the forced response of the at-
94 mospheric circulation, near-surface air temperature and snow accumulation in the West
95 Antarctic over the past decades, and, second, at isolating the individual contributions
96 from the greenhouse gas increase and stratospheric ozone depletion on the climate changes.
97 To this end, we perform a detection and attribution analysis (D&A), in order to sepa-
98 rate the observed climate changes into two components: a component related to inter-
99 nal variability of the climate system, and another related to changes in the anthropogenic
100 and natural forcings (Hegerl & Zwiers, 2011). This allows us to assess the anthropogenic
101 influence on the ongoing surface climate changes occurring in the West Antarctic since
102 the mid-20th century. To do so, we employ new existing instrumental and proxy-based
103 reconstructions and two LEs of ESM simulations.

104 **2 Methods**

105 **2.1 Observations and reconstructions**

106 Although some atmospheric pressure observations span the past century, the vast
107 majority start at best in 1958 (Turner et al., 2004). To put the recent changes in a broader
108 context and identify the potential long-term effect of the forcing, we thus need to rely
109 on reconstructions based on paleo proxies (for instance ice core data), which provide ro-

110 bust sea-level pressure reconstructions over the past few centuries. In this study, we use
111 the sea-level pressure reconstruction covering the 1800–2000 CE time period from Dalaiden
112 et al. (2021) who dynamically constrain the climate evolution in the West Antarctic sec-
113 tor with ice core snow accumulation and isotopic content proxy data along with tree ring
114 width records within a data assimilation framework. When compared with observations
115 over the satellite era, this reconstruction shows good skill (Dalaiden et al., 2021; O’Connor
116 et al., 2021). For near-surface air temperature, the instrumental-based reconstruction
117 from Nicolas and Bromwich (2014) that spans the 1958–2012 CE time period is employed.
118 This reconstruction shows a good agreement with independent observations and is con-
119 sidered as the reference temperature reconstruction for the second half of the 20th cen-
120 tury. Finally, for snow accumulation, we use the well-evaluated reconstruction of Medley
121 and Thomas (2019), which uses the combination of ice core snow accumulation records
122 with atmospheric reanalysis to ensure spatial coherence.

123 **2.2 Climate model simulations**

124 LEs are ideal for detection and attribution studies as a large number of model sim-
125 ulations is required to reduce the noise associated with internal variability. In this study,
126 we use two LEs performed with two different ESMs, which also include several additional
127 experiments driven by different forcing combinations. The first LE has been performed
128 with the Coupled Earth System Model version 1 (CESM1) (Kay et al., 2015). CESM1-
129 LE consists of 35 ensemble members covering the 1920–2080 CE period and are driven
130 by the historical forcing until 2005 CE and the Representative Concentration Pathway
131 (RCP) 8.5 afterwards (CMIP5 forcings). In addition to the 35 historical ensemble mem-
132 bers, Deser, Phillips, et al. (2020) conducted additional experiments of 20 ensemble mem-
133 bers to isolate the impacts of GHG and anthropogenic aerosols (AER). More specifically,
134 these two specific-forcing LEs follow the same protocol as for the historical LE but the
135 forcing (i.e., the greenhouse gases or anthropogenic aerosols) is set at the 1920 CE level
136 throughout the simulation (i.e., all-but-one-forcing). These two ensembles are referred
137 to as xGHG and xAER, respectively. Along with these two all-but-one-forcing LEs, Landrum
138 et al. (2017) provided an ensemble of eight ensemble members following the same pro-
139 tocol as xGHG and xAER but with the stratospheric ozone concentration fixed at the
140 1955 CE level (referred to as xO3). For deriving the GHG, O3 and AER ensembles from
141 the ALL, xGHG, xAER and xO3 ensembles, we follow the procedure of Deser, Phillips,

142 et al. (2020). Numerous studies have shown that CESM1 simulates relatively well the
143 climate around the Antarctic when compared with regional climate models and obser-
144 vations (e.g., Lenaerts et al., 2016; Dalaiden et al., 2021; England et al., 2016; Landrum
145 et al., 2017), which gives confidence in the use of CESM1 for this study.

146 In addition to CESM1, we also employ a second LE performed with the ESM CanESM2
147 (Arora et al., 2011; Kirchmeier-Young et al., 2017). This LE is available over 1950–2100
148 CE. This LE contains four experiments of 50 ensemble members with different forcings.
149 As in the case of CESM1, an experiment driven by the historical forcing from 1950 un-
150 til 2005 CE and by the RCP8.5 forcing from 2005 CE is available. The three other ex-
151 periments consist of single-forcing experiments: natural (solar and volcanic forcings; NAT),
152 AER and O3. In contrast with CESM1, the single-forcing experiments are performed
153 by keeping all the forcings constant except the forcing of interest throughout the sim-
154 ulation. As in Swart et al. (2018), we estimate the response to the anthropogenic green-
155 house gases by subtracting the responses of all of the single-forcing experiments from the
156 response of the experiment with all forcings. Although CanESM2 has been less analyzed
157 than CESM1 in the Antarctic, this model has been recently used to identify the forced
158 drivers of the surface changes in the Southern Ocean over the 20th century (Swart et al.,
159 2018; Hobbs et al., 2021).

160 **2.3 Detection and attributions analysis**

161 We first associate the evolution of a climate variable with a specific forcing by com-
162 paring the trends over the past decades in the all-forcing experiment (ALL) and a single-
163 forcing experiment. This simple analysis allows us to give a first estimate of the role of
164 a specific forcing on the total simulated response. In addition, we conduct a D&A anal-
165 ysis (Ribes & Terray, 2013) on the atmospheric circulation, surface air temperature and
166 snow accumulation in the West Antarctic sector over the 1950 CE post period. As per
167 Hegerl and Zwiers (2011), we consider that the detection is successful when the observed
168 change is outside of the range of internal variability of the climate system and the at-
169 tribution as assigning a change to a specific forcing. The method used in thus study is
170 detailed in Section S1 (Supporting Information).

171 The D&A analysis is performed on the ASL index (computed as the average sea-
172 level pressure over 170–290°E, 75–60°S as in Hosking et al. (2013)), West Antarctic near-

173 surface air temperature and snow accumulation. For temperature and snow accumula-
174 tion, the four regional time-series (see Figure S1 for the definitions of the regions) are
175 included in the regression to increase the probability to detect a change by including the
176 spatial component. The analysis period is 1950–2000 CE for the ASL and snow accu-
177 mulation, and 1959–2012 CE for temperature. These periods reflect the periods covered
178 by both the observations and climate model simulations.

179 **3 Results**

180 **3.1 Observed and simulated surface climate changes since the mid-20th** 181 **century**

182 Figure 1 a shows the annual evolution of the ASL index in the proxy-based recon-
183 struction of Dalaiden et al. (2021) and as simulated in CESM1-LE and CanESM2-LE
184 over 1950–2080 CE. Both the reconstruction and climate model simulations display a deep-
185 ening of the ASL over the second half of the 20th century, which is consistent with pre-
186 vious studies (Thomas et al., 2015; Dalaiden et al., 2021; O’Connor et al., 2021). The
187 reconstructed trend over 1951–2000 CE is in the range of the simulated trends (Figure
188 1 b; -0.40 hPa per decade vs -0.26 ± 0.18 hPa per decade (mean \pm std) and -0.30 ± 0.17
189 hPa per decade for CESM1-LE and CanESM2-LE, respectively; all statistically signif-
190 icant at the 95% level). Both CESM1-LE and CanESM2-LE suggest a further deepen-
191 ing of the ASL for the end of the 21st century but at a lower rate: -0.22 ± 0.16 hPa per
192 decade and -0.18 ± 0.14 hPa per decade over 2031–2080 CE, respectively.

193 Figure 2 presents maps of the observed linear trends of sea-level pressure, near-surface
194 air temperature and snow accumulation along with the forced response from the ALL
195 experiment for CESM1-LE and CanESM2-LE over 1959–2000 CE. While the reconstruc-
196 tion shows a deepening of the ASL and an increased anticyclonic situation around the
197 Drake Passage and Weddell Sea, the deepening of the ASL present in the total forced
198 trend from the two models is rather embedded in a Southern Annular Mode (SAM)-dominated
199 response (i.e., observations are more zonally asymmetric than the forced response). This
200 is not a contradictory result since the ensemble mean is dominated by the forced response
201 with the internal variability reduced (by averaging over the ensemble members). Indeed,
202 some ensemble members display a pattern similar to the reconstruction (Figures S1 and
203 S2). We therefore argue that the difference in the trend between the reconstruction and

204 ensemble means mainly comes from the contribution of internal variability present in the
 205 reconstruction but that is reduced in the model ensemble means.

206 The signal observed in the near-surface air temperature over 1959–2000 CE is char-
 207 acterized by a large warming over the Antarctic Peninsula ($0.35^{\circ}\text{C decade}^{-1}$ [p-value<0.05])
 208 and the Central WAIS ($0.31^{\circ}\text{C decade}^{-1}$ [p-value<0.05]; Figure 2 and Table S1; see Fig-
 209 ure S1 for the definitions of the regions). The forced response of the ALL experiment
 210 displays a more homogeneous surface warming pattern, albeit both CESM1-LE and CanESM2-
 211 LE show the strongest warming in the Antarctic Peninsula ($0.21^{\circ}\text{C decade}^{-1}$ [p-value<0.05]
 212 and $0.35^{\circ}\text{C decade}^{-1}$ [p-value<0.05], respectively) and underestimate the warming in
 213 the Central WAIS ($0.11^{\circ}\text{C decade}^{-1}$ [p-value<0.05] and $0.16^{\circ}\text{C decade}^{-1}$ [p-value<0.05],
 214 respectively). Finally, we observe a good agreement between observed and forced sim-
 215 ulated snow accumulation changes over 1959–2000 CE (Figure 2). Both the Medley and
 216 Thomas (2019) reconstruction and models display a snow accumulation increase over the
 217 Antarctic Peninsula, and the Eastern and Central WAIS: for those three regions taken
 218 together the observations give a trend of $35.22\text{ Gt decade}^{-1}$ against $14.86\text{ Gt decade}^{-1}$
 219 for CESM1-LE and $11.95\text{ Gt decade}^{-1}$ for CanESM2-LE (all statistically significant at
 220 the 95% level). For Western WAIS, a statistically significant snow accumulation decrease
 221 is observed ($-9.29\text{ Gt decade}^{-1}$), in contrast with the two models that show no significant
 222 change (Table S1). For both temperature and snow accumulation, some ensemble mem-
 223 bers are in better agreement with the reconstruction (especially regarding the magni-
 224 tude of change; Figures S4-S7) indicating a substantial role of internal variability in the
 225 observed changes.

226 **3.2 Detection and attribution to individual forcings**

227 Figure 3 presents the contribution of the increased greenhouse gas and stratospheric
 228 ozone depletion to the sea-level pressure, near-surface air temperature and snow accu-
 229 mulation trends from CESM1-LE and CanESM2-LE over 1959–2000 CE. Stratospheric
 230 ozone depletion and greenhouse gases are the main drivers of the deepening ASL over
 231 1959–2000 CE in both models, since the forced trend patterns of sea-level pressure from
 232 these two forcings are very similar to the total forced trend pattern (Figure 3). The strato-
 233 spheric ozone depletion experiments display a $-0.25\text{ hPa decade}^{-1}$ (p-values<0.01) and
 234 $-0.16\text{ hPa decade}^{-1}$ (p-values<0.01) trend for CESM1-LE and CanESM2-LE respectively,
 235 while the greenhouse gases experiments show $-0.18\text{ hPa decade}^{-1}$ (p-values<0.01) and

236 -0.19 hPa decade⁻¹ (p-values<0.01) trend for CESM1-LE and CanESM2-LE respectively
237 (Table S1).

238 In contrast with the atmospheric circulation, the greenhouse gas forcing explains
239 most of the total forced pattern of the near-surface air temperature trend over 1959–2000
240 CE (Figure 3) while the stratospheric ozone depletion forcing is associated with no sta-
241 tistically significant surface temperature changes for West Antarctica in both models (Ta-
242 ble S1). However, it is worth noting that the stratospheric ozone depletion forcing leads
243 to surface warming in the Antarctic Peninsula (Table S1). Furthermore, the GHG spa-
244 tial pattern of trends in near-surface air temperature is relatively homogeneous compared
245 with the O3 spatial pattern (Figure 3). As for snow accumulation, our analysis indicates
246 that both the greenhouse gases and stratospheric ozone depletion are responsible for the
247 observed snow accumulation changes (Figure 3). Furthermore, in the two models, the
248 spatial fingerprint of the stratospheric ozone depletion forcing on the snow accumula-
249 tion trends is more heterogeneous than the one related to the greenhouse gas forcing.
250 The former is associated with more pronounced trends that are in opposition between
251 the Antarctic Peninsula, Eastern and Central WAIS, and the Western WAIS. This pat-
252 tern is typically related to the influence of the ASL (Dalaiden et al., 2021) and there-
253 fore explains the substantial role of stratospheric ozone depletion on the snow accumu-
254 lation changes.

255 Results from the formal D&A analysis (section 2.3) are displayed in Figure 4. Both
256 CESM1-LE and CanESM2-LE show that an impact of all forcings on changes in the ASL,
257 near-surface air temperature and snow accumulation over the past decades is detected,
258 since the scaling factors (including the confidence intervals) are different from zero (Fig-
259 ure 4). The observed changes cannot be thus explained by internal variability. There-
260 fore, according to our results, changes in the forcings are responsible for the recent sur-
261 face climate changes in the West Antarctic. It is worth noting that the confidence in-
262 tervals are the largest for the ASL. This could suggest that, although the impact of the
263 forcings on the ASL is detected, internal variability plays an important role in the ASL
264 variability compared with the other two variables.

265 Regarding the attribution to specific forcings, both models show a detectable re-
266 sponse to the greenhouse gas forcing for near-surface air temperature and snow accumu-
267 lation, since the scaling factors are different from zero (Figure 4). In contrast with CESM1-

268 LE, the greenhouse gas forcing is also detected for the ASL in CanESM2-LE. However,
269 when extending the period to 1940–2000 CE, results from CESM1-LE also display a de-
270 tection of the greenhouse gas forcing on the ASL (not shown). In addition to the green-
271 house gas forcing, CESM1-LE indicates that the impact of stratospheric ozone depletion
272 on the ASL and snow accumulation is also detectable. The scaling factor is relatively
273 high, which could be explained by the fact that stratospheric ozone depletion is not dom-
274 inant all year long but primarily during the austral summer (Thompson et al., 2011).
275 Regarding near-surface air temperature, the scaling factor for stratospheric ozone deple-
276 tion is statistically different from zero. However, the high scaling factor value suggests
277 that, while the observed pattern resembles the ozone signal, the amplitude of the sim-
278 ulated signal is too small to confidently attribute it to this forcing. Finally, according
279 to CanESM2-LE results, the natural forcing (probably volcanic eruptions) is also detected
280 in temperature and snow accumulation changes. For all the analyzed variables, the ALL
281 forcings results show clear detection of a forced signal (since scaling factors generally in-
282 clude unity), but the attribution to a specific forcing is less clear.

283 **4 Discussion and conclusions**

284 Our results are directly impacted by several sources of uncertainties. Since we use
285 the D&A analysis to detect forced signal in the observed time-series, any errors in that
286 time-series may impact the scaling factors, and therefore potentially our ability to de-
287 tect and attribute the observed changes. Yet, the observational network is sparse in Antarc-
288 tica. For instance, the instrumental-based near-surface air temperature reconstruction
289 of Nicolas and Bromwich (2014) is only based on four records situated in West Antarc-
290 tica. Additionally, for the ASL and snow accumulation, we had to rely on the reconstruc-
291 tions based on paleo records, which are known to be more prone to uncertainties than
292 instrumental records. Although the information on the uncertainty is available, directly
293 considering account it in the D&A framework is challenging. However, we note that these
294 proxy-based reconstructions are well evaluated against state-of-the-art observations (Dalaiden
295 et al., 2021; Medley & Thomas, 2019), which thus gives confidence in our results. Fur-
296 thermore, the estimations of the forced responses depend on the climate model, and there-
297 fore the model biases may impact the conclusions. However, here, we have analyzed two
298 models developed by two different groups from which we generally obtained the same
299 conclusions.

300 While considering these limitations, our results robustly show that the annual deep-
301 ening of the ASL, surface warming and snow accumulation increase in West Antarctica
302 since the 1950s are out of the range of internal variability and can be attributed to the
303 anthropogenic forcing. In agreement with previous studies that concluded for a forced
304 response of the ASL during the austral summer due to anthropogenic forcing, and in par-
305 ticular to stratospheric ozone depletion over about 1965–2005 CE (England et al., 2016;
306 Fogt & Zbacnik, 2014), we argue that the deepening ASL over 1950–2000 CE can be only
307 explained on the annual basis by changes in the forcings. Furthermore, as for near-surface
308 air temperature, a previous study (i.e., Smith & Polvani, 2017) found that the West Antarc-
309 tic surface warming over the past decades is not out of the range of internal variability.
310 However, we argue that our findings are not in contradiction with their results. Smith
311 and Polvani (2017) focused on the 1960–2005 CE period, while our analysis is performed
312 on a longer period (i.e., 1959–2012 CE). According to Smith and Polvani (2017), a forced
313 anthropogenic signal emerges when analyzing temperature changes over a longer period.
314 The probability density distributions of the 46-year and 54-year temperature trends from
315 the control pre-industrial simulation of CESM1 (Figure S8) indicate that the observed
316 1959–2012 CE temperature trend is out of the range of internal variability (>99.9th per-
317 centile), in contrast with the 1960–2005 CE trend (<99.9th percentile). Additionally, Smith
318 and Polvani (2017) analyzed all available model simulations, regardless of their perfor-
319 mance in simulating the Antarctic climate and did not use an optimal fingerprinting method,
320 which would have better handled the role of internal variability on observed changes (sim-
321 ilar conclusions are obtained with CanESM2 [Figure S9]). Finally, the detection of sur-
322 face warming is consistent with the findings of Gillett et al. (2008) who showed that the
323 atmospheric warming at the two poles is due to human activities.

324 The detection of snow accumulation changes is less robust than for temperature
325 and ASL since the scaling factors including confidence intervals are greater than unity,
326 especially for CanESM2-LE. This means that the models underestimate the amplitude
327 of change. Unlike sea-level pressure and temperature, snow accumulation strongly varies
328 in space, making a successful detection more challenging. The coarse resolution of the
329 ESMs – which fails to represent small spatial scale processes –, missing processes in ESMs
330 along with the uncertainties in ice core records are likely to blame. However, Medley and
331 Thomas (2019) showed that 80% of the variance in spatial snow accumulation trends over
332 1957–2000 CE are explained by the positive SAM trend – yet the ASL is strongly related

333 to the SAM (Turner et al., 2009; Hosking et al., 2013). Furthermore, the general atmo-
334 spheric warming may be the primary driver of the 20th century Antarctic snow accu-
335 mulation increase (Medley & Thomas, 2019; Dalaiden et al., 2020). Since changes in the
336 ASL and temperature can be attributed to forcings according to our results and previ-
337 ous studies (England et al., 2016; Fogt & Zbacnik, 2014; Gillett et al., 2008), we believe
338 that our snow accumulation results are not an artefact.

339 Both CESM1-LE and CanESM2-LE agree on the important role of the greenhouse
340 gas forcing on these changes occurring in the West Antarctic. The detection of the green-
341 house gas forcing on those climate changes can be related to physical mechanisms high-
342 lighted in previous studies. Higher greenhouse gas concentrations strengthen the tem-
343 perature gradient between the mid and high latitudes, which results in intensifying the
344 westerly jet (e.g., Arblaster & Meehl, 2006), and therefore the deepening ASL (e.g., Fogt
345 & Marshall, 2020). Yet, the ASL strongly modulates the surface climate in West Antarc-
346 tica (e.g., Raphael et al., 2016) by enhancing the southerly flow towards the Eastern WAIS
347 and Antarctic Peninsula, including the intrusions of moist and warm air in these regions.
348 In contrast, the Western WAIS is less prone to these intrusions for years with strong ASL
349 (Fogt et al., 2012; Fyke et al., 2017). This results in surface warming in Eastern WAIS
350 and the Antarctic Peninsula, and surface cooling in the Western WAIS (Marshall & Thomp-
351 son, 2016). Over the Antarctic Peninsula and Eastern and Central WAIS, an overall pos-
352 itive correlation between atmospheric temperature and snow accumulation is noticed (Cavitte
353 et al., 2020). In these regions, when warm, moist air from the ocean is brought to the
354 continent by the ASL, air moisture content precipitates due to the orographic lifting, lead-
355 ing to more snow accumulation in these regions. Because the air has lost almost all of
356 its humidity content during adiabatic uplift, Western WAIS experiences a snow accu-
357 mulation deficit due to the ASL deepening, strengthening the Eastern/Western snow ac-
358 cumulation dipole (Dalaiden et al., 2021). Furthermore, the greenhouse gas forcing leads
359 to a uniform surface warming, which agrees with Bindoff et al. (2013). This explains,
360 for instance, the surface warming observed in the Central and Western WAIS that can-
361 not be explained by the ASL deepening.

362 Furthermore, our results based on CESM1-LE indicate that stratospheric ozone de-
363pletion is the primary driver of the deepening ASL over the second half of the 20th cen-
364 tury (followed by the greenhouse gas forcing). This forcing impacts the atmospheric cir-
365 culation without destabilizing the global energy budget directly (Thompson et al., 2011),

366 in contrast with the greenhouse gas forcing. By primarily modifying wind patterns, partly
367 through the ASL, stratospheric ozone depletion leads to a more pronounced dipole be-
368 tween the Western WAIS/Antarctic Peninsula and the Eastern WAIS for both near-surface
369 air temperature and snow accumulation. Therefore, we confirm previous findings on the
370 major role of this forcing on the recent snow accumulation increase (Lenaerts et al., 2018;
371 Chemke et al., 2020) and more generally on the ASL (England et al., 2016; Fogt & Zbac-
372 nik, 2014). In contrast with these studies, we formally performed a D&A analysis to an-
373alyze the forced response to the stratospheric ozone depletion. It worth noting that the
374 role of stratospheric ozone depletion in CanESM2 is less clear than in CESM1 since only
375 the greenhouse gas forcing is detected in the D&A analysis. However, the forced atmo-
376 spheric circulation changes associated with stratospheric ozone depletion in CanESM2
377 suggests a substantial contribution from this forcing.

378 In summary, our study shows that the overall observed ASL, near-surface air tem-
379 perature and, with slightly lower confidence, snow accumulation changes over the past
380 decades can be attributed to the greenhouse gas and, in some cases, stratospheric ozone
381 depletion forcings. Therefore, we could expect that these changes will continue in the
382 coming decades because of the increasing greenhouse gas concentrations. However, thanks
383 to the Montreal Protocol (Kuttippurath & Nair, 2017) aiming to decrease the substances
384 responsible for stratospheric ozone depletion, the recovery of the stratospheric ozone layer
385 could mitigate the impact of the greenhouse gas forcing. The ozone recovery would lead
386 to a more anticyclonic situation in the West Antarctic (i.e., decreased deepening ASL).
387 As a weaker ASL tends to reduce glacier thinning (Dotto et al., 2020), this atmospheric
388 situation could have major implications for the global sea-level rise by decreasing the con-
389 tribution of the Antarctic Ice Sheet.

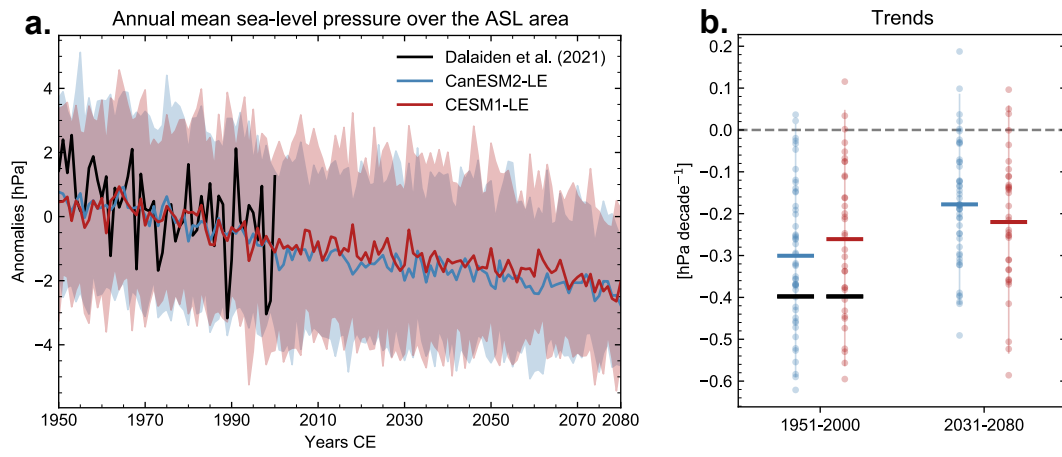


Figure 1. (a) Annual reconstructed (i.e., Dalaiden et al. (2021)) and simulated (CESM1-LE and CanESM2-LE) sea-level pressure over the Amundsen Sea Low area (in hPa) over 1950–2080 CE. The shaded areas correspond to the 5th and 95th percentiles of the model ensemble. (b) Linear trends over the 1951–2000 CE and 2031–2080 CE periods are displayed. The color dots correspond to the trend for each ensemble member and the horizontal thick coloured line corresponds to the ensemble mean. The horizontal thick black line is the observed trend.

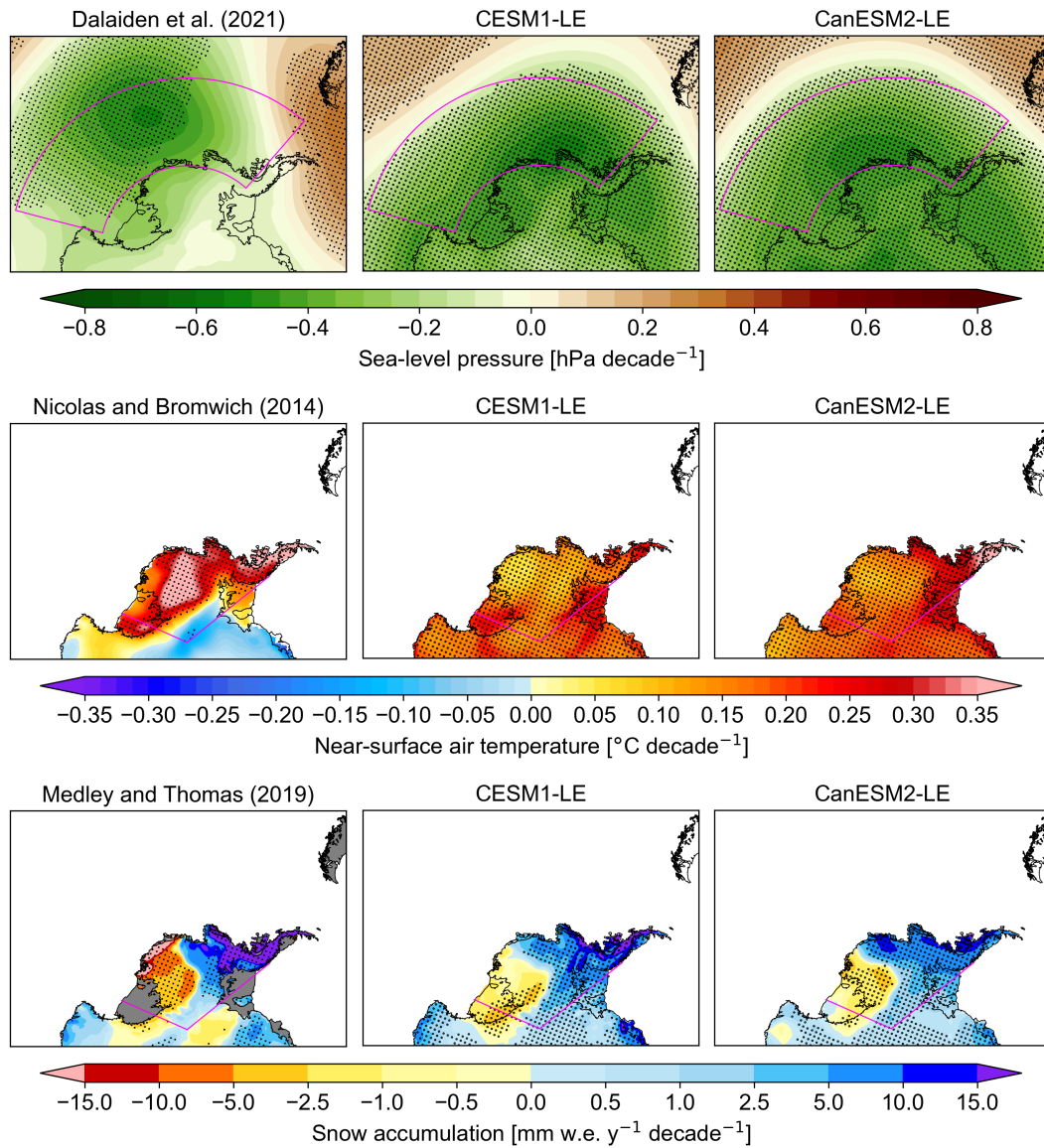


Figure 2. Reconstructed and simulated (CESM1-LE and CanESM2-LE) linear trends in sea-level pressure (hPa decade^{-1}), near-surface air temperature ($^{\circ}\text{C decade}^{-1}$) and snow accumulation ($\text{mm w.e. y}^{-1} \text{decade}^{-1}$) over 1959–2000 CE. The reconstructed sea-level pressure corresponds to the paleo-based reconstruction of Dalaiden et al. (2021), while for snow accumulation, the ice core-based reconstruction of Medley and Thomas (2019) is displayed. The near-surface air temperature reconstruction is from the reconstruction of Nicolas and Bromwich (2014), which is based on instrumental records. The simulated trends correspond to the ensemble mean of the CESM1-LE and CanESM2-LE all forcing experiments (30 and 50 ensemble members, respectively). Stippling indicates statistical significant trends (95% confidence). For sea-level pressure, the magenta box corresponds to the area on which the Amundsen Sea Low index is computed. Magenta lines displayed in near-surface air temperature and snow accumulation maps correspond to the limits of West Antarctica.

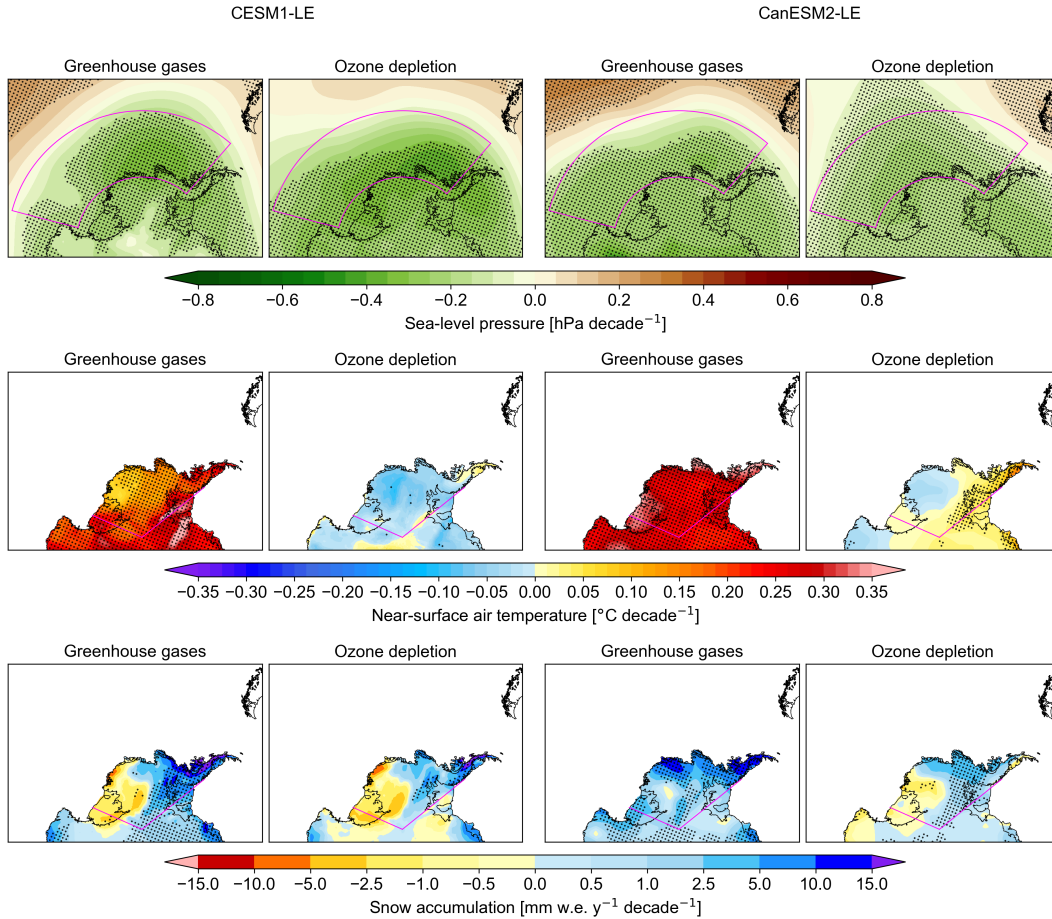


Figure 3. Annual linear trends for sea-level pressure (hPa decade^{-1}), near-surface air temperature ($^{\circ}\text{C decade}^{-1}$) and snow accumulation ($\text{mm w.e. y}^{-1} \text{ decade}^{-1}$) from the ensemble mean greenhouse gases and ozone depletion experiments performed with CESM1 and CanESM2 over 1959–2000 CE. Stippling indicates statistically significant trends at 95% level. For sea-level pressure, the magenta box corresponds to the area on which the Amundsen Sea Low index is computed. Magenta lines displayed in near-surface air temperature and snow accumulation maps correspond to the limits of West Antarctica.

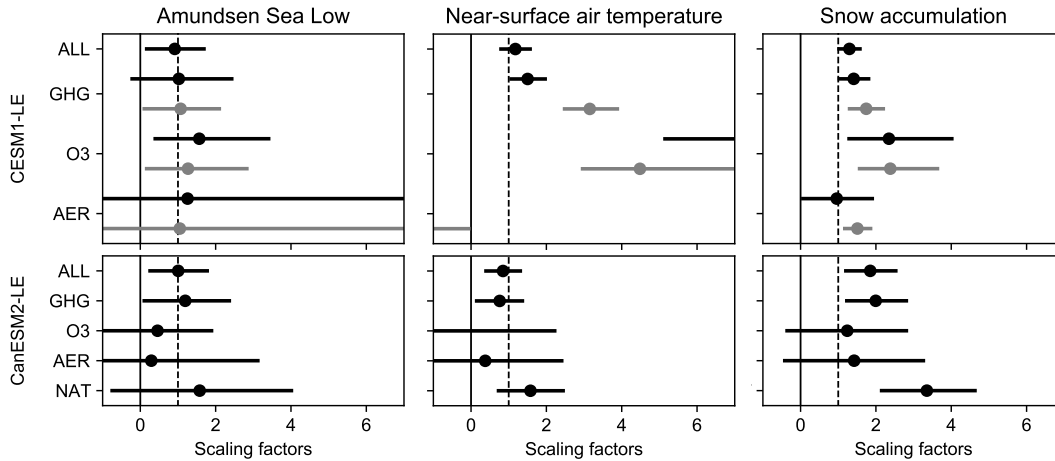


Figure 4. Detection and attribution scaling factors for the mean sea-level pressure over the Amundsen Sea Low area over 1950–2000 CE, near-surface air temperature over 1959–2012 CE and snow accumulation over 1950–2000 CE in West Antarctica for CESM1-LE (top) and canESM2-LE (bottom). The ASL proxy-based reconstructions of (Dalaiden et al., 2021) and the snow accumulation proxy-based reconstruction of (Medley & Thomas, 2019) are used as observations in the D&A analysis while the instrumental-based reconstruction of (Nicolas & Bromwich, 2014) is used for near-surface air temperature. As for CESM1-LE, the scaling factors for GHG, O3 and AER are displayed in black and the scaling factors for all-but-the specific forcing are shown in grey. Due to model output availability, the D&A analysis using the stratospheric ozone depletion ensemble of CESM1 is performed over 1955–2000 CE for the ASL and snow accumulation, and 1959–2005 CE for near-surface air temperature. Error bars correspond to the 90% confidence intervals. All the data are annual averages.

5 Data Availability Statement

The near-surface air temperature reconstruction of Nicolas and Bromwich (2014) can be downloaded at http://polarmet.osu.edu/datasets/Antarctic_recon/. The paleo snow accumulation reconstruction of Medley and Thomas (2019) is available at <https://earth.gsfc.nasa.gov/cryo/data/antarctic-accumulation-reconstructions> while the reconstruction of the atmospheric circulation from Dalaiden et al. (2021) is archived on Zenodo (<https://zenodo.org/record/4770179#.YmbEtC8Rr0o>). The CESM1 and CanESM2 data used in this study are freely available through <https://www.earthsystemgrid.org> and <https://data-donnees.ec.gc.ca>, respectively.

Acknowledgments

We thank William Hobbs and an anonymous reviewer for their constructive comments, which greatly helped to improve our manuscript. QD is a Research Fellow within the F.R.S.-FNRS (Belgium). G.H. and A.S. were funded by the NERC project GloSAT (NE/S015698/1). A.S. further received funding from a Chancellors fellowship at the University of Edinburgh. HG is a Research Director within the F.R.S.-FNRS (Belgium). This work was partly supported by the Belgian Research Action through Interdisciplinary Networks (BRAIN-be) from the Belgian Science Policy Office in the framework of the project “East Antarctic surface mass balance in the Anthropocene: observations and multiscale modelling (Mass2Ant)” (contract no. BR/165/A2/Mass2Ant).

References

- Arblaster, J. M., & Meehl, G. A. (2006). Contributions of external forcings to southern annular mode trends. *Journal of Climate*, *19*(12), 2896–2905. doi: 10.1175/JCLI3774.1
- Arora, V. K., Scinocca, J. F., Boer, G. J., Christian, J. R., Denman, K. L., Flato, G. M., ... Merryfield, W. J. (2011). Carbon emission limits required to satisfy future representative concentration pathways of greenhouse gases. *Geophysical Research Letters*, *38*(5), 3–8. doi: 10.1029/2010GL046270
- Bindoff, N. L., Stott, P. A., AchutaRao, K. M., Allen, M. R., Gillett, N., Gutzler, D., ... Zhang, X. (2013). Detection and attribution of climate change: From global to regional. In T. F. Stocker et al. (Eds.), *Climate change 2013: The physical science basis. contribution of working group i*

- 421 to the fifth assessment report of the intergovernmental panel on climate
422 change (pp. 867–952). Cambridge, UK: Cambridge University Press. doi:
423 10.1017/CBO9781107415324.022
- 424 Cavitte, M., Dalaiden, Q., Goosse, H., Lenaerts, J., & Thomas, E. (2020). Rec-
425 onciling the surface temperature–surface mass balance relationship in models
426 and ice cores in Antarctica over the last two centuries. *The Cryosphere*, *14*,
427 4083–4102. doi: 10.5194/tc-2020-36
- 428 Chemke, R., Previdi, M., England, M. R., & Polvani, L. M. (2020). Distinguishing
429 the impacts of ozone and ozone-depleting substances on the recent increase
430 in Antarctic surface mass balance. *Cryosphere*, *14*(11), 4135–4144. doi:
431 10.5194/tc-14-4135-2020
- 432 Connolley, W. M. (1997). Variability in annual mean circulation in southern high
433 latitudes. *Climate Dynamics*, *13*(10), 745–756. doi: 10.1007/s003820050195
- 434 Dalaiden, Q., Goosse, H., Lenaerts, J. T., Cavitte, M. G., & Henderson, N. (2020).
435 Future Antarctic snow accumulation trend is dominated by atmospheric
436 synoptic-scale events. *Communications Earth & Environment*, *1*, 1–9. Re-
437 trieved from <http://dx.doi.org/10.1038/s43247-020-00062-x> doi:
438 10.1038/s43247-020-00062-x
- 439 Dalaiden, Q., Goosse, H., Rezsöhazy, J., & Thomas, E. R. (2021). Reconstruct-
440 ing atmospheric circulation and sea-ice extent in the west antarctic over the
441 past 200 years using data assimilation. *Climate Dynamics*, *57*(11), 3479–
442 3503. Retrieved from <https://doi.org/10.1007/s00382-021-05879-6> doi:
443 10.1007/s00382-021-05879-6
- 444 Deser, C., Lehner, F., Rodgers, K. B., Ault, T., Delworth, T. L., DiNezio, P. N.,
445 ... Ting, M. (2020). Insights from Earth system model initial-condition
446 large ensembles and future prospects. *Nature Climate Change*, *10*(4), 277–
447 286. Retrieved from <http://dx.doi.org/10.1038/s41558-020-0731-2> doi:
448 10.1038/s41558-020-0731-2
- 449 Deser, C., Phillips, A. S., Simpson, I. R., Rosenbloom, N., Coleman, D., Lehner,
450 F., ... Stevenson, S. (2020). Isolating the evolving contributions of an-
451 thropogenic aerosols and greenhouse gases: A new CESM1 large ensem-
452 ble community resource. *Journal of Climate*, *33*(18), 7835–7858. doi:
453 10.1175/JCLI-D-20-0123.1

- 454 Dotto, T. S., Naveira Garabato, A. C., Wåhlin, A. K., Bacon, S., Holland,
455 P. R., Kimura, S., . . . Jenkins, A. (2020). Control of the Oceanic Heat
456 Content of the Getz-Dotson Trough, Antarctica, by the Amundsen Sea
457 Low. *Journal of Geophysical Research: Oceans*, *125*(8). Retrieved from
458 <https://doi.org/10.1029/2020JC016113> doi: 10.1029/2020JC016113
- 459 England, M. R., Polvani, L. M., Smith, K. L., Landrum, L., & Holland, M. M.
460 (2016). Robust response of the Amundsen Sea Low to stratospheric
461 ozone depletion. *Geophysical Research Letters*, *43*(15), 8207–8213. doi:
462 10.1002/2016GL070055
- 463 Fogt, R. L., & Marshall, G. J. (2020). The Southern Annular Mode: Variability,
464 trends, and climate impacts across the Southern Hemisphere. *WIREs Climate*
465 *Change*, *n/a*(*n/a*), e652. Retrieved from <https://doi.org/10.1002/wcc.652>
466 doi: 10.1002/wcc.652
- 467 Fogt, R. L., Schneider, D. P., Goergens, C. A., Jones, J. M., Clark, L. N., & Gar-
468 beroglio, M. J. (2019). Seasonal Antarctic pressure variability during the twen-
469 tieth century from spatially complete reconstructions and CAM5 simulations.
470 *Climate Dynamics*, *53*(3), 1435–1452. Retrieved from [http://dx.doi.org/](http://dx.doi.org/10.1007/s00382-019-04674-8)
471 [10.1007/s00382-019-04674-8](http://dx.doi.org/10.1007/s00382-019-04674-8) doi: 10.1007/s00382-019-04674-8
- 472 Fogt, R. L., Wovrosh, A. J., Langen, R. A., & Simmonds, I. (2012). The charac-
473 teristic variability and connection to the underlying synoptic activity of the
474 Amundsen-Bellinghousen Seas Low. *Journal of Geophysical Research Atmo-*
475 *spheres*, *117*(7), 1–22. doi: 10.1029/2011JD017337
- 476 Fogt, R. L., & Zbacnik, E. A. (2014). Sensitivity of the Amundsen sea low to strato-
477 spheric ozone depletion. *Journal of Climate*, *27*(24), 9383–9400. doi: 10.1175/
478 JCLI-D-13-00657.1
- 479 Fyke, J., Lenaerts, J. T., & Wang, H. (2017). Basin-scale heterogeneity in Antarc-
480 tic precipitation and its impact on surface mass variability. *Cryosphere*, *11*(6),
481 2595–2609. doi: 10.5194/tc-11-2595-2017
- 482 Gillett, N. P., Arora, V. K., Matthews, D., & Allen, M. R. (2013). Con-
483 straining the ratio of global warming to cumulative CO2 emissions us-
484 ing CMIP5 simulations. *Journal of Climate*, *26*(18), 6844–6858. doi:
485 10.1175/JCLI-D-12-00476.1
- 486 Gillett, N. P., Stone, D. A., Stott, P. A., Nozawa, T., Karpechko, A. Y., Hegerl,

- 487 G. C., ... Jones, P. D. (2008). Attribution of polar warming to human influ-
488 ence. *Nature Geoscience*, *1*(11), 750–754. doi: 10.1038/ngeo338
- 489 Hegerl, G., & Zwiers, F. (2011). Use of models in detection and attribution of cli-
490 mate change. *Wiley Interdisciplinary Reviews: Climate Change*, *2*(4), 570–591.
491 doi: 10.1002/wcc.121
- 492 Hobbs, W. R., Roach, C., Roy, T., Sallée, J.-B., & Bindoff, N. (2021). Anthro-
493 pogenic temperature and salinity changes in the southern ocean. *Journal of*
494 *Climate*, *34*(1), 215 - 228. Retrieved from [https://journals.ametsoc.org/](https://journals.ametsoc.org/view/journals/clim/34/1/jcliD200454.xml)
495 [view/journals/clim/34/1/jcliD200454.xml](https://journals/clim/34/1/jcliD200454.xml) doi: 10.1175/JCLI-D-20-0454
496 .1
- 497 Hosking, J. S., Orr, A., Marshall, G. J., Turner, J., & Phillips, T. (2013). The influ-
498 ence of the amundsen-bellingshausen seas low on the climate of West Antarc-
499 tica and its representation in coupled climate model simulations. *Journal of*
500 *Climate*, *26*(17), 6633–6648. doi: 10.1175/JCLI-D-12-00813.1
- 501 IPCC. (2019). IPCC Special Report on the Ocean and Cryosphere in a Chang-
502 ing Climate [H.-O. Pörtner, D.C. Roberts, V. Masson-Delmotte, P. Zhai, M.
503 Tignor, E. Poloczanska, K. Mintenbeck, A. Alegría, M. Nicolai, A. Okem, J.
504 Petzold, B. Rama, N.M. Weyer (eds.)]. *In press*.
- 505 Jones, J. M., Gille, S. T., Goosse, H., Abram, N. J., Canziani, P. O., Charman,
506 D. J., ... Vance, T. R. (2016). Assessing recent trends in high-latitude
507 Southern Hemisphere surface climate. *Nature Climate Change*, *6*(10), 917–
508 926. Retrieved from <http://dx.doi.org/10.1038/nclimate3103> doi:
509 10.1038/nclimate3103
- 510 Kay, J. E., Deser, C., Phillips, A., Mai, A., Hannay, C., Strand, G., ... Vertenstein,
511 M. (2015). The community earth system model (CESM) large ensemble
512 project : A community resource for studying climate change in the presence of
513 internal climate variability. *Bulletin of the American Meteorological Society*,
514 *96*(8), 1333–1349. doi: 10.1175/BAMS-D-13-00255.1
- 515 Kirchmeier-Young, M. C., Zwiers, F. W., & Gillett, N. P. (2017). Attribution of ex-
516 treme events in Arctic Sea ice extent. *Journal of Climate*, *30*(2), 553–571. doi:
517 10.1175/JCLI-D-16-0412.1
- 518 Kuttippurath, J., & Nair, P. J. (2017). The signs of Antarctic ozone hole recovery.
519 *Scientific Reports*, *7*(1), 1–8. Retrieved from <http://dx.doi.org/10.1038/>

- 520 s41598-017-00722-7 doi: 10.1038/s41598-017-00722-7
- 521 Landrum, L. L., Holland, M. M., Raphael, M. N., & Polvani, L. M. (2017). Strato-
522 spheric Ozone Depletion: An Unlikely Driver of the Regional Trends in
523 Antarctic Sea Ice in Austral Fall in the Late Twentieth Century. *Geophysi-
524 cal Research Letters*, *44*(21), 11,062–11,070. doi: 10.1002/2017GL075618
- 525 Lenaerts, J. T., Fyke, J. G., & Medley, B. (2018). The signature of ozone de-
526 pletion in recent Antarctic precipitation change: a study with the Commu-
527 nity Earth System Model. *Geophys. Res. Lett.*, *45*, 12931—12939. doi:
528 10.1029/2018GL078608
- 529 Lenaerts, J. T., Vizcaino, M., Fyke, J., van Kampenhout, L., & van den Broeke,
530 M. R. (2016). Present-day and future Antarctic ice sheet climate and surface
531 mass balance in the Community Earth System Model. *Climate Dynamics*,
532 *47*(5-6), 1367–1381. doi: 10.1007/s00382-015-2907-4
- 533 Maher, N., Milinski, S., & Ludwig, R. (2021). Large ensemble climate model
534 simulations: introduction, overview, and future prospects for utilising multi-
535 ple types of large ensemble. *Earth System Dynamics*, *12*(2), 401–418. Re-
536 trieved from <https://esd.copernicus.org/articles/12/401/2021/> doi:
537 10.5194/esd-12-401-2021
- 538 Marshall, G. J., & Thompson, D. W. (2016). The signatures of large-scale patterns
539 of atmospheric variability in Antarctic surface temperatures. *Journal of Geo-
540 physical Research*, *121*(7), 3276–3289. doi: 10.1002/2015JD024665
- 541 Marshall, G. J., Thompson, D. W., & van den Broeke, M. R. (2017). The Signa-
542 ture of Southern Hemisphere Atmospheric Circulation Patterns in Antarctic
543 Precipitation. *Geophysical Research Letters*, *44*(22), 11,580–11,589. doi:
544 10.1002/2017GL075998
- 545 Medley, B., & Thomas, E. R. (2019). Increased snowfall over the Antarctic Ice Sheet
546 mitigated twentieth-century sea-level rise. *Nature Climate Change*, *9*(1), 34–
547 39. Retrieved from <http://dx.doi.org/10.1038/s41558-018-0356-x> doi:
548 10.1038/s41558-018-0356-x
- 549 Nicolas, J. P., & Bromwich, D. H. (2014). New reconstruction of antarctic near-
550 surface temperatures: Multidecadal trends and reliability of global reanalyses.
551 *Journal of Climate*, *27*(21), 8070–8093. doi: 10.1175/JCLI-D-13-00733.1
- 552 O'Connor, G. K., Steig, E. J., & Hakim, G. J. (2021). Strengthening Southern

- 553 Hemisphere Westerlies and Amundsen Sea Low Deepening Over the 20th Cen-
554 tury Revealed by Proxy-Data Assimilation. *Geophysical Research Letters*,
555 48(24). doi: 10.1029/2021gl095999
- 556 Raphael, M. N., Marshall, G. J., Turner, J., Fogt, R. L., Schneider, D., Dixon,
557 D. A., ... Hobbs, W. R. (2016). The Amundsen sea low: Variability, change,
558 and impact on Antarctic climate. *Bulletin of the American Meteorological*
559 *Society*, 97(1), 111–121. doi: 10.1175/BAMS-D-14-00018.1
- 560 Ribes, A., & Terray, L. (2013). Application of regularised optimal fingerprinting
561 to attribution. Part II: Application to global near-surface temperature. *Climate*
562 *Dynamics*, 41(11-12), 2837–2853. doi: 10.1007/s00382-013-1736-6
- 563 Smith, K. L., & Polvani, L. M. (2017). Spatial patterns of recent Antarctic surface
564 temperature trends and the importance of natural variability: lessons from
565 multiple reconstructions and the CMIP5 models. *Climate Dynamics*, 48(7-8),
566 2653–2670. doi: 10.1007/s00382-016-3230-4
- 567 Steig, E. J., Schneider, D. P., Rutherford, S. D., Mann, M. E., Comiso, J. C., &
568 Shindell, D. T. (2009). Warming of the Antarctic ice-sheet surface since
569 the 1957 International Geophysical Year. *Nature*, 457(7228), 459–462. doi:
570 10.1038/nature07669
- 571 Swart, N. C., Gille, S. T., Fyfe, J. C., & Gillett, N. P. (2018). Recent Southern
572 Ocean warming and freshening driven by greenhouse gas emissions and ozone
573 depletion. *Nature Geoscience*, 11(11), 836–841. Retrieved from [http://](http://dx.doi.org/10.1038/s41561-018-0226-1)
574 dx.doi.org/10.1038/s41561-018-0226-1 doi: 10.1038/s41561-018-0226-1
- 575 Thomas, E. R., Hosking, J. S., Tuckwell, R. R., Warren, R. A., & Ludlow, E. C.
576 (2015). Twentieth century increase in snowfall in coastal West Antarc-
577 tica. *Geophysical Research Letters*, 42(21), 9387–9393. doi: 10.1002/
578 2015GL065750
- 579 Thompson, D. W. J., Solomon, S., Kushner, P. J., England, M. H., Grise, K. M.,
580 & Karoly, D. J. (2011). Signatures of the Antarctic ozone hole in Southern
581 Hemisphere surface climate change. *Nature Geoscience*, 4(11), 741–749. Re-
582 trieved from <http://www.nature.com/doifinder/10.1038/ngeo1296> doi:
583 10.1038/ngeo1296
- 584 Turner, J., Colwell, S. R., Marshall, G. J., Lachlan-Cope, T. A., Carleton, A. M.,
585 Jones, P. D., ... Iagovkina, S. (2004). The SCAR READER project: Toward

- 586 a high-quality database of mean Antarctic meteorological observations. *Jour-*
 587 *nal of Climate*, 17(14), 2890–2898. doi: 10.1175/1520-0442(2004)017<2890:
 588 TSRPTA>2.0.CO;2
- 589 Turner, J., Colwell, S. R., Marshall, G. J., Lachlan-Cope, T. A., Carleton, A. M.,
 590 Jones, P. D., ... Iagovkina, S. (2005). Antarctic climate change during the last
 591 50 years. *International Journal of Climatology*, 25(3), 279-294. Retrieved from
 592 <https://rmets.onlinelibrary.wiley.com/doi/abs/10.1002/joc.1130>
 593 doi: <https://doi.org/10.1002/joc.1130>
- 594 Turner, J., Comiso, J. C., Marshall, G. J., Lachlan-Cope, T. A., Bracegirdle, T.,
 595 Maksym, T., ... Orr, A. (2009). Non-annular atmospheric circulation change
 596 induced by stratospheric ozone depletion and its role in the recent increase
 597 of Antarctic sea ice extent. *Geophysical Research Letters*, 36(8), 1–5. doi:
 598 10.1029/2009GL037524

599 Supporting References

- 600 Allen, M. R., & Stott, P. A. (2003). Estimating signal amplitudes in optimal finger-
 601 printing, part I: Theory. *Climate Dynamics*, 21(5-6), 477–491. doi: 10.1007/
 602 s00382-003-0313-9
- 603 Gillett, N. P., Kirchmeier-Young, M., Ribes, A., Shiogama, H., Hegerl, G. C.,
 604 Knutti, R., ... Ziehn, T. (2021). Constraining human contributions to ob-
 605 served warming since the pre-industrial period. *Nature Climate Change*, 11(3),
 606 207–212. Retrieved from <https://doi.org/10.1038/s41558-020-00965-9>
 607 doi: 10.1038/s41558-020-00965-9
- 608 Ribes, A., Planton, S., & Terray, L. (2013). Application of regularised optimal fin-
 609 gerprinting to attribution. Part I: Method, properties and idealised analysis.
 610 *Climate Dynamics*, 41(11-12), 2817–2836. doi: 10.1007/s00382-013-1735-7
- 611 Tett, S. F., Stott, P. A., Allen, M. R., Ingram, W. J., & Mitchell, J. F. (1999).
 612 Causes of twentieth-century temperature change near the Earth’s surface.
 613 *Nature*, 399(6736), 569–572. doi: 10.1038/21164